Proceedings of the
International Conference on Mechanical Engineering and Renewable Energy 2017
(ICMERE2017) 18 – 20 December, 2017, Chittagong, Bangladesh

ICMERE2017-PI-325

NUMERICAL SIMULATION OF EFFECTS OF REYNOLDS NUMBER ON NON-NEWTONIAN BLOOD FLOW WITH SPIRAL COMPONENT THROUGH A REGULAR STENOSED ARTERY

Md Alamgir Kabir[1], **Md Ferdous Alam**[2] **and Md. Ashraf Uddin**[1]

[1]Department of Mathematics, Shahjalal University of Science and Technology, Sylhet, Bangladesh
[2]Department of Mechanical Engineering, Shahjalal University of Science and Technology, Sylhet, Bangladesh

Joy_sust123@yahoo.com, mfalam-mee@sust.edu*, auddin-mat@sust.edu

Abstract- *Numerical simulation of blood flow through arterial stenosis can play crucial role in biofluid studies, as it is a complex flow phenomenon because of its Non-Newtonian behavior. In the present study, the Carreau model has been used to investigate the characteristics of blood flow through a regular stenosis. The effects of Reynolds number (Re) on Non-Newtonian blood flow through a 3D model of a biological type arterial stenosis is examined. The geometry of a regular stenosis has been established by researching previous studies. The standard k-ω model is used for simulation of blood flow for different Reynolds numbers (Re = 500, 1000, 1500, 2000). Some numerical results such as velocity profile, pressure outlet, streamline, wall shear stress (WSS), turbulent kinetic energy (TKE) etc. are examined for different spiral velocities at different Reynolds numbers. Details investigation and significant pathological issues are described throughout the investigation.*

Keywords: Non-Newtonian, Stenosis, Reynolds number, Blood flow, Wall shear

1. INTRODUCTION

Nowadays congenital and complication of cardiovascular disease has become one of the vital issues of morbidity and mortality in the recent humanity. Blood circulation is one of the most important functions of human body and blood vessels are called the high ways of human body. Blood vessels that carry oxygen-rich blood to the heart and other parts of the body are called arteries which have smooth inner walls and blood flows through them easily without any obstacles.

Arterial stenosis is an unusual narrowing of an artery where cholesterol and other lipids are deposited in the inner lining of the arterial wall and the cross-sectional area of a blood vessel shrinks. When the depositions of fat and other lipids build up in the beneath artery walls it causes repeated injury to the inner lining of the arteries which results in physical stress in the form of high blood pressure or inflammatory stress, infections, high cholesterol or high blood glucose. When arteries have blockage caused by these types of diseases, it is called atherosclerosis or arteriosclerosis vascular disease (ASVD) Ross et.al. [1]. Such kind of disease is promoted by Low-Density Lipoproteins (LDL) without adequate removal of fats and cholesterol from the macrophages by functional High-Density Lipoproteins (HDL). When the increasing of fatty material which becomes almost settled in the artery forms a thickened area in the vessel wall called plaque, it reduces the effective cross-section of the vessel and slows down the blood flow. The rupturing of this plaque exposes the fatty core and can lead to the formation of a thrombus, where the blood platelets form a clot about the exposed area which can block off the entire artery and it becomes very dangerous when it obstructs or stop the flow of blood to some major organs, such as the heart or brain that may be the cause of sudden death.

As hemodynamic behavior of the blood flow in arterial stenosis bears some important aspects for medical applications It is therefore no doubt that this topic is now of major concern to the community and the focus of numerous research efforts and more recently, computational techniques have demonstrated the ability to model flow behavior in stenosed arteries with different geometries and conditions that can be specified according to the actual conditions. A thorough understanding of blood dynamics in human vessels has a great interest among the researcher and nowadays the computational simulation is playing a significant role in this field. Therefore a large number of computational and experimental studies have been conducted to simulate and investigate blood flow in arterial stenosis. The hemodynamic factors such as wall pressure and shear stress have major effects in damaging and weakening the internal wall of the artery at the post-stenotic turbulent region. For example, high-wall shear stress associated with turbulence has a significant effect on vascular

endothelial injury Fry DL [2]. In some cases, they over-stimulate platelet thrombosis, and then accelerate atherosclerosis, as reported by Stein et al. [3]. On the other hand, the thickening of the intima caused by remodeling of the vessel wall is related to the presence of low shear stress at the throat of the stenosis, Ku et al. [4]. Using laser Doppler anemometry and flow visualization techniques, Ahmed and Giddens [5] studied the effect of axisymmetric stenosis on the velocity field in the post-stenosis zone in various percentages. In the experiment, the upstream flow remained stable, the study considered the Reynolds number in the range of 500-2000. Ghalichi et al. [6] used the k-ω of Wilcox turbulence model to study the blood flow in the same stenotic arterial model as in [5]. Their results show that the k-ω model have a good agreement with experimental data and is superior to the standard k-ε model in predicting blood pressure and turbulence intensity. Lee et al. [7] studied the turbulence flow through a series of axisymmetric stenosis by applying a stable parabolic profile at the upstream, indicating that the k-ω model has good accuracy for predicting laminar as well as turbulence flow through stenosed artery and more stenoses can result in a lower critical Reynolds number that means an earlier occurrence of turbulence for the stenotic flows. Paul et al. [8] used Large–Eddy simulation (LES) techniques to study pulsatile blood flow through a 3D model of a biological type stenosis formed on the top wall. The smooth constriction, which was generated using the cosine relation of [5], gives a fairly accurate representation of an arterial stenosis and their results shows that the high level of flow recirculation associated with complex patterns of transient blood flow have a significant contribution to the generation of the turbulent fluctuations found in the post-stenosis region.The limitation of the k–ω model in the modelling of transient blood flow through the stenosis is also highlighted in their study. Sarifuddin et al. [9] used three differently shaped stenoses-cosine form, irregular shape and smooth constriction and investigated the blood flow through them numerically prescribing a parabolic velocity profile at the inlet and shows that the post-stenotic results has a good agreement with existing investigations in the steady state but mainly influenced by the choice of the stenosis used in the model.

The circular motion of the heart pump causes the blood to pulsate naturally through the arteries. The blood flow in the circulatory system is mainly pulsatile laminar flow. However, due to the combined action of flow pulsation and strong shear, flow separation, recirculation, and stenotic recanalization, the passage of blood vessels through severe stenos is can lead to periodic transitions in the posterior stenos is to turbulence.As the heart twisting on its own axis the blood flow through artery is spiral that is obvious from the vivo research of Stonebridge and Brophy [10] and Stonebridge et al. [11] which has a theoretical advantage- forward, rotation-induced stability and lateral force reduction can reduce turbulence and stenosis in the conical branch arterial tree and have a beneficial effect on the mechanism of endothelial damage and repair.

In the this study, the Carreau model has been used to model the non-newtonian flow. Four different Reynolds numbers (Re = 500, 1000, 1500, 2000) and corresponding spiral velocities have been used in this study of investigate the effect of Re.

2. PROBLEM SPECIFICATION

It is obvious that one of the crucial parts of blood flow simulation is the problem specification and formation for proper investigation. An artificial geometrical model of the stenosis considered as the conventionally used cosine curve in the blood vessel shown in Fig. 1(a) is created using the following formula [5].

$$\frac{r(Z)}{R} = 1 - \delta_c\left[1 + \cos\left(\frac{Z\pi}{D}\right)\right], \quad -D \le Z \le D \tag{1}$$

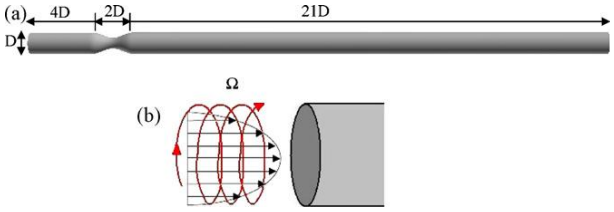

Fig.1: (a) Schematic of the model of a stenosed blood vessel and (b) an interpretation of the spiral boundary condition with the parabolic flow at the inlet of the model. [12]

Where, *r* and *Z* are the radial and axial co-ordinates and *R* and *D* are the radius and diameter of the unstenosed vessel respectively and the percentage of the stenosis is control by the parameter δ_c.The constrictions followed the cosine curve with 75% area reductions. The smooth reduction of the cross-sectional area produced inside the vessel using Eq. (1) provides a fairly accurate representation of the biological form of arterial stenosis as it has been employed previously in theoretical calculations by [5],Deshpande et al. [13] and Smith et al. [14]. The entire span of the biological form model is taken as 540(27*D*) mm [5], where diameter *D*=20 mm and the length of the upstream, downstream and stenosed zone are taken as 4*D*, 21*D and 2D* respectively. Blood flow through the model is considered as incompressible and Newtonian and homogeneous fluid [15] with a density of $\rho = 1060\ kg/m^3$ and a constant dynamic viscosity of $\mu = 3.71 \times 10^{-3}$ Pa s. At the inlet of the model a spiral boundary condition along with a parabolic velocity profile is used which is shown in Fig. 1(b).

The Navier–Stokes equations are used as the governing equations of motion of the blood flow and after applying the Reynolds time-averaging techniques, the Reynolds averaged Navier–Stokes (RANS) are obtained and written in the tensor form as [16],

$$\frac{\partial \mathrm{u_i}}{\partial \mathrm{x_i}} = 0 \tag{2}$$

$$\frac{\partial}{\partial t}(\rho u_i) + \frac{\partial}{\partial x_j}(\rho u_i u_j) = -\frac{\partial p}{\partial x_i} + \frac{\partial}{\partial x_j}\left[\mu\left(\frac{\partial u_i}{\partial x_j} + \frac{\partial u_j}{\partial x_i}\right)\right] + \frac{\partial \tau_{ij}}{\partial x_j} \tag{3}$$

. where u_i are the mean velocity components along the

Cartesian co-ordinate systems, $x_i = (x, y, z)$, p is the pressure and τ_{ij} are the Reynolds stresses which are modeled employing the Boussinesq hypothesis as,

$$\tau_{ij} = -\rho\langle u_i' u_j' \rangle = \mu_t \left(\frac{\partial u_i}{\partial x_j} + \frac{\partial u_j}{\partial x_i} \right) - \frac{2}{3}\rho k \delta_{ij} \quad (4)$$

Where u_i' are the fluctuating velocity components; $k = \frac{1}{2}\langle u_i' u_j' \rangle$ is the turbulent kinetic energy and μ_t is the turbulent eddy-viscosity obtained by employing the standard $k-\omega$ model of Wilcox [17]. The eddy-viscosity is modeled as,

$$\mu_t = \frac{\rho k}{\omega} \quad (5)$$

where ω is the specific dissipation rate. The following modelled transport equations (Wilcox [17]) are solved to obtain k and ω:

$$\frac{\partial k}{\partial t} + \frac{\partial k(u_j)}{\partial x_j} = -\frac{1}{\rho}(\rho u_i' u_j') \frac{\partial (u_i)}{\partial x_j} - \beta^* k\omega + \frac{\partial}{\partial x_j}\left[\frac{1}{\rho}(\mu + \sigma^* \mu_t) \frac{\partial k}{\partial x_j} \right] \quad (6)$$

$$\frac{\partial \omega}{\partial t} + \frac{\partial \omega(u_j)}{\partial x_j} = -\alpha_1 \frac{\omega}{\partial k}(\rho u_i' u_j') \frac{\partial (u_i)}{\partial x_j} - \beta\omega^2 + \frac{\partial}{\partial x_j}\left[\frac{1}{\rho}(\mu + \sigma \mu_t) \frac{\partial \omega}{\partial x_j} \right] \quad (7)$$

Where $\sigma^* = 0.5$, $\beta^* = 0.072$, $\sigma = 0.5$, $\alpha 1 = 1.0$ and $\beta = 0.072$.
The details of this turbulent model can be found in [15,16].

3.1 Boundary Condition and Computational Procedure

The artery that has been used in the existing model is considering as an inflexible and impervious circular tube with a no-slip boundary condition for fluid having zero velocity ($u_i = 0$) relative to the boundary along with a parabolic velocity profile –

$$v(x, y) = 2V\left[1 - \left(\frac{r}{R}\right)^2\right] \quad (8)$$

which has been imposed at the inlet of the model, where V is the bulk streamwise velocity related to the Reynolds number, $Re = \rho VD/\mu$, of the blood flow. The spiral velocity (Ω) is characterized as a proportion of the forward velocity inside the blood-vessel that has been calculated with the following equation

$$\Omega = \frac{V}{R} C \quad (9)$$

In which C=1/6 as mentioned in [17, 18] is a constant that governs the magnitude of the spiral speed. Additionally, the outlet of the model has been treated as a pressure outlet using the default setting for the gauge pressure to become zero at the outlet. Commercially available CFD software, Fluent [16], has been used in this study. This software uses finite volume method for discretization. The finite volume method represents and evaluates partial differential equations in the form of algebraic equations. Pressure based solver has been used to solve the flow eqations with implicit formulation method. Additionally, the SIMPLE scheme for pressure-velocity coupling has been used. In the discretisation process, the second order upwind scheme is used for the equations of momentum, turbulent kinetic energy (k) and specific dissipation rate (ω); while the second order accurate scheme is used for the Poisson-like pressure equation. The inlet boundary conditions for the stream wise velocity has been written in C-language using the interface of User Defined Function (UDF) of Fluent and linked with the solver. The solution process is initiated using arbitrary values of the velocity components and k-ω, and their residuals are monitored at every iteration. The magnitude of the residuals dropped gradually, which is a strong indicator for the stable and accurate solutions, and the iteration process is stopped when the residuals are leveled off at 10^{-6} (in fact the residuals became independent to the iteration number at this level) and the final converged solutions are achieved. Finally this study has been carried out for three different mesh numbers and grid independent test was conducted.

Table 1: Values of spiral velocity (Ω) for the different Reynolds numbers

Re	C	$\Omega(rad/s)$
0	1/6	0.0
500		1.46
1000		2.92
1500		4.38
2000		5.83

4. RESULTS AND DISCUSSION

In the present study, axial velocity is used as comparing variables for grid independence and the results are shown in Fig.2(a), Fig.2(b) and Fig.2(c) for different grid points. Initially, Grid 1 consists of 50630 cells, and then it was increased by about 99% for Grid 2 that consists of 100630 cells. Finally, Grid 3 was increased by a huge amount (more than 323% including 229680 cells) for the entire computational area. This grid independence test has been performed to ensure that the numerical solutions are independent on the choice of the grid arrangements.

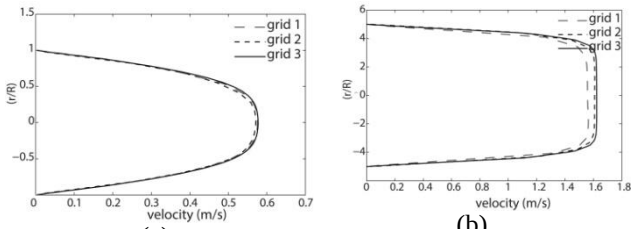

(a) (b)

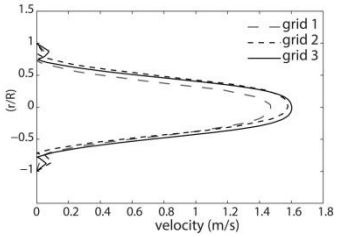

(c)

Fig.2: Grid independence test shown for axial velocity at different radial positions (a) Z=-2D (b) Z=0D (c)Z=2D

4.1 Effect on Pressure

The effect of the spiral flow on the total pressure at the centre of the model artery has been stuied (Fig.3). A large pressure drop occurs at 0m axial position, which is the position of the stenosis. However, pressure remains almost constant from 0.1m to the rest of the artery. For larger Re (Re=2000) a slight increase in pressure in the post stenotic region can be observed.

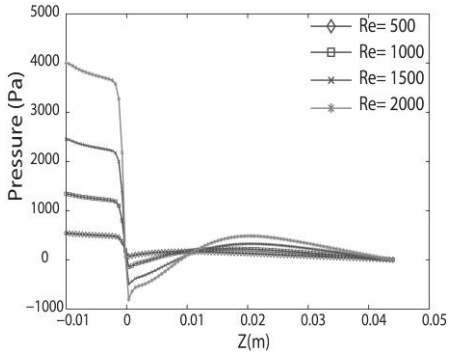

Fig.3: Centerline total pressure at various axial positions for different Reynolds numbers

4.2 Effect on Velocity

Centerline velocities (Fig. 4) have also been studied to investigate the effect of Reynolds. The effect of spiral component can be explained in these figures. From Table.1 it can be observed that for a higher Re, spiral velocity also increases. With the increase in Re and Ω, magnitude of axial velocity also increases. Due to the stenosis there is a large increase in axial velocity magnitude. The effect of spiral component, however, is quite less on radial and tangential velocity although For lower Re (Re=500,1000) the effect is significant. For comparatively higher Reynolds numbers and gradually higher Ω the effect is not that mentionable.

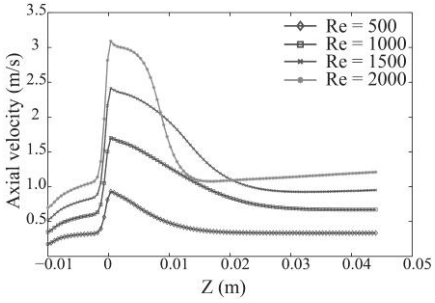

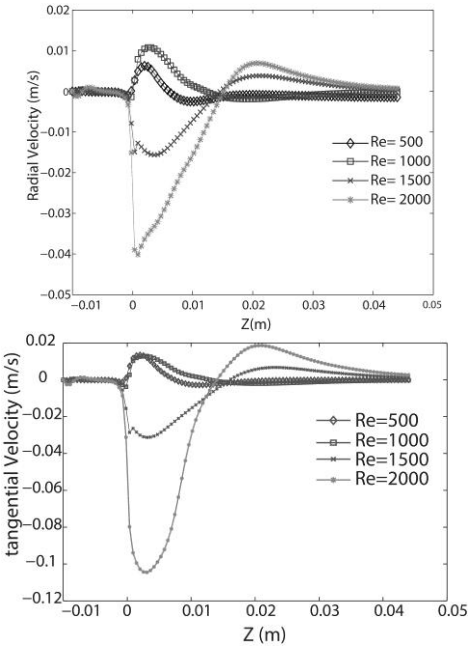

Fig.4: Centerline velocity at different axial positions for different Reynolds numbers

Velocity profiles for different Reynolds number has been shown in Fig.5. A dimensionless parameter (r/R) has been taken on the y-axis. From the figure it is obvious that the magnitude of velocity is maximum at the stenosis and almost 0.9 m/s, 1.6 m/s, 2.3 m/s, 3 m/s for Re= 500, 1000, 1500, 2000 respectively. The parabolic velocity profile before the stenosis also depicts the intial condition, the shape of which changed drastically after the stenosis.

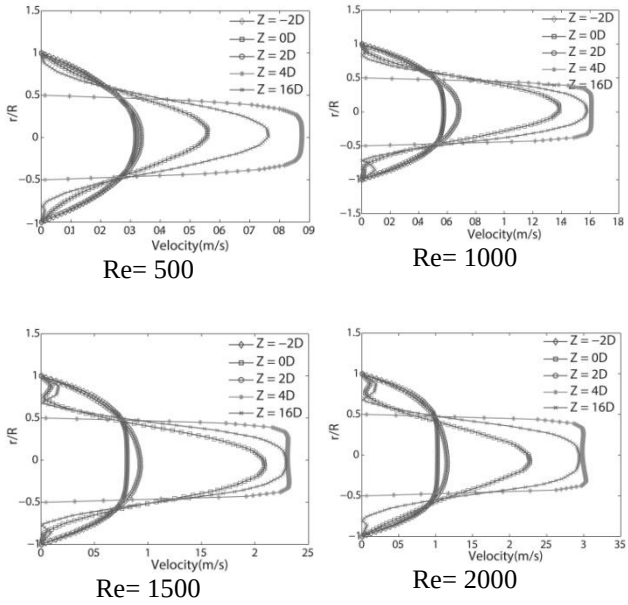

Fig.5: Velocity profiles for different Reynolds number

4.3 Effect on Wall Shear Stress

The influence of spiral flow on the wall shear stress has been elaborat3ed in Fig.6. It can be easily seen that, with the increase in Reynolds number (which means increment in spiral flow) wall shear stress along the pipe

wall increases. The contour of wall shear stress is easily observable. Also at the stenotic region the change in shear stress is significant. When Ω = 5.83 rad/sec, maximum wall shear stress is observed.

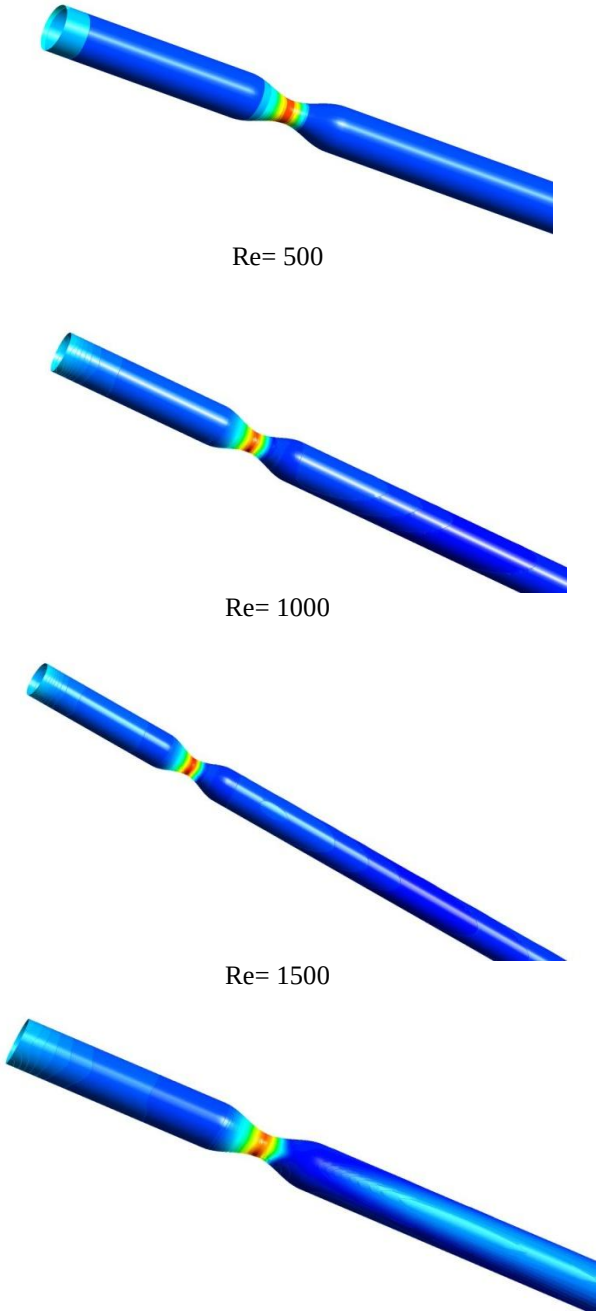

Fig.6: Wall shear stress along the pipe wall

The effect of spiral flow can be described efficiently form the cross sectional views of the velocity streamlines. From Fig.7, the structure of the blood flow at the downstream for different spiral speeds can be investigated. Interestingly, they produce twisted three dimensional flow. This pattern of flow is similar to that of the MRI measurement of the blood flow in a patient's artery with thrombosis done by Frydrychowicz et al. [19].

The intensity of the twisting flow at 4D distance is quite strong and flow pattern is much chaotic in the downstream region. This chaotic behavior can cause potential damage to blood cells and inner surface of the artery [12].

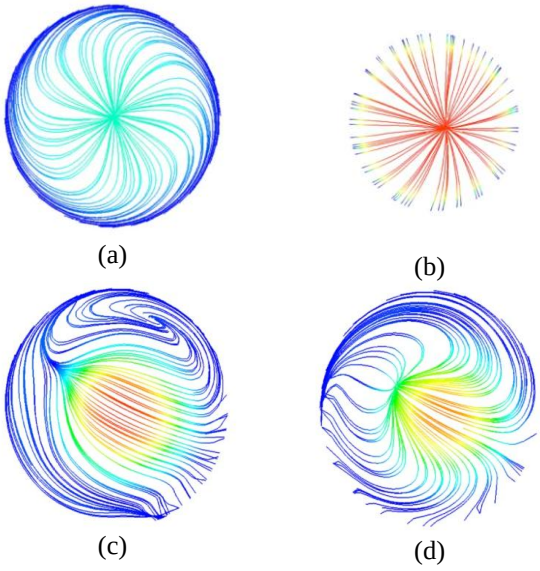

Fig.7: Cross section of velocity streamlines at (a) Z=-2D (b) Z=0D (c) Z=2D (d) Z=4D

4.4 Effect on Turbulence Kinetic Energy

The effect of the Reynolds number on the turbulent kinetic energy (TKE) has been shown in Fig.8. The increase of TKE for Re= 2000 is quite phenomenal compared to other Reynolds numbers, while the effect for Re=500, 1000 can be almost negligible. There is significant increment of TKE in the downstream (in the post stenosis region).

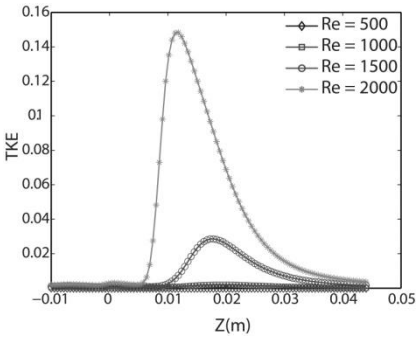

Fig.8: Turbulence kinetic energy at different axial positions for different Reynolds numbers

5. CONCLUSION

The increase in turbulence kinetic energy in the downstream region is responsible for the destruction of blood cells, and the platelets in the blood are activated, resulting in many pathologic diseases attack in human body. The turbulent kinetic energy is reduced by the spiral flow as it causes rotational stability in the forward flow as a results it prevents the damage of blood cell which is a beneficial effect. At the same time, the spiral

flow in the posterior stenosis in the oscillation wall shear stress, which is harmful. In this paper a simplified model of artery has been used. Further research should be conducted in this regard to investigate the proper biological boundary conditions. This paper aims to draw decisive conclusion that spiral component of blood flow has important impact on human artery while the Reynolds number play a crucial role for significant parameters of blood flow.

6. ACKOWLEDGEMENT

The first author is grateful to the Ministry of Science and Technology, Government of Bangladesh for NST fellowship 2016-2017 which partially supported to carry out this study.

7. REFERENCES

[1] R. Ross, "The pathogenesis of atherosclerosis: a perspective for the 1990s", *Nature*, vol. 362, no. 6423, pp. 801–809, 1993.

[2] D. L. Fry, "Acute vascular endothelial changes associated with increased blood velocity gradients", *Circulation Research*, vol. 22, pp. 165–97, 1968.

[3] P. D. Stein, F. J. Walburn, and H. N. Sabbah, "Turbulent stresses in the region of aortic and pulmonary valves", ***Journal of Biomechanical Engineering***, vol. 104, no. 3, pp. 238–44, 1982.

[4] D. N. Ku, D. P. Giddens, C. K. Zarins, and S. Glagov, "Pulsatile flow and atherosclerosis in the human carotid bifurcation", *Arteriosclerosis, Thrombosis, and Vascular Biology*, vol. 5, no. 3, pp. 293–302, 1985.

[5] S. A. Ahmed, and D. P. Giddens, "Velocity measurements in steady flowthrough axisymmetric stenoses at moderate Reynolds number", *Journal of Biomechanic*s, vol. 16, no. 7, pp. 505–16, 1983.

[6] F. Ghalichi, X. Deng, A. Champlan, Y. Douville, M. King, and R. Guidoin, "Low Reynolds number turbulence modelling of blood flow in arterial stenosis", *Biorheology*, vol. 35, no. 4-5, pp. 281–4, 1998.

[7] T. S. Lee, W. Liao, and H. T. Low, "Numerical simulation of turbulent flow through series stenoses", *Internation Journal for Numerical Methods in Fluids*, vol. 42, no. 7, pp. 717–40, 2003.

[8] M. C. Paul, M. M. Molla, and G. "Roditi, Large–Eddy simulation of pulsatile blood flow", *Medical Engineering and Physics*, vol. 31, no. 1, pp. 153–9, 2009.

[9] Sarifuddin, S. Chakravarty, P. K. and Mandal, G. C. Layek. "Numerical simulation of unsteady generalized Newtonian blood flow through differently shaped distensible arterial stenoses", *Journal of Medical Engineering & Technology*, vol. 32, no. 5, pp. 385–99, 2008.

[10] P. A. Stonebridge, and C. M. Brophy, "Spiral laminar flow in arteries?", *Lancet*, vol. 338, no. 8779, pp. 1360–1, 1991.

[11] P. A. Stonebridge, P. E. Hoskins, P. L. Allan, and F. F. Belch, "Spiral laminar flow in vivo", *Clinical Science*, vol. 91, no. 1, pp. 17–21, 1996.

[12] M. C. Paul, and A. Larman. "Investigation of spiral blood flow in a model of arterial stenosis." *Medical Engineering & Physics*, vol. 31, no. 9, 1195-1203, 2009.

[13] M. D. Deshpande, D. P. Giddens, and R. F. Mabon, "Steady laminar flow through modelled vascular stenoses", *Journal of Biomechanics*, vol. 9, no. 4, pp. 165-l 74, 1976.

[14] F. T. Smith, "On entry-flow effects in bifurcating blocked or constricted tubes", *Journal of Fluid Mechanics*, vol. 78, pp. 709-736, 1976.

[15] D. N. Ku, "Blood flows in arteries", *Annual Review in Fluid Mechanics*, vol. 29, pp. 399–434, 1997.

[16] FLUENT. 15, Tutorials Guide. USA: Fluent INC; 2007.

[17] D. C. Wilcox, *Turbulence modelling for CFD*, La Canada California: DWC Industries, 1993.

[18] P. A. Stonebridge, C. Buckley, A. Thompson, J. Dick, G. Hunter, and J. A. Chudek, "Non spiral and spiral (helical) flow patterns in stenoses: in vitro observations using spin and gradient echo magnetic resonance imaging (MRI) and computational fluid dynamic modeling", *International Angiology*, vol. 23, no. 3, pp. 276-283, 2004.

[19] A. Frydrychowicz, A. Harloff, J. Bernd, Z Maxim, W. Ernst, A. B. Thorsten, L. Mathias, H. Jürgen, and M. Michae, "Time-resolved, 3-dimensional magnetic resonance flow analysis at 3 T: visualization of normal and pathological aortic vascular hemodynamics", *Journal of Computer Assisted Tomography*, vol. 31, no. 1, pp. 9-15, 2007.

8. NOMENCLATURE

Symbol	Meaning	Unit
D	Artery diameter	m
ρ	Density	kg/m^3
r	Radial location from axis of artery	m
μ	Dynamic viscosity	Ns/m^2
V	Stream wise bulk velocity	m/s
v	Instantaneous velocity	m/s
Ω	Spiral velocity	rad/sec
Re	Reynolds number	Dimensionless
R	Radius of blood vessel	m
k	Turbulent kinetic energy	J/kg
μ_t	Turbulent eddy-viscosity	m^2/sec
ω	Specific dissipation rate	$1/s$
u_i	Mean velocity components	m/s
u_i'	Fluctuating velocity components	m/s
C	Constant	Dimensionless